Structures and Acid−Base Properties of La/Al_2O_3 − Role of La Addition to Enhance Thermal Stability of γ-Al_2O_3

Takashi Yamamoto, Takaki Hatsui, Takahiro Matsuyama, Tsunehiro Tanaka,* and Takuzo Funabiki

Department of Molecular Engineering, Kyoto University, Kyoto 615-8510, Japan

Received August 6, 2003. Revised Manuscript Received September 29, 2003

Structures and acid−base properties of La/Al_2O_3 with different La loadings and calcination temperatures were examined by surface-area measurements, catalyses, IR, XRD, and La K-edge XAFS spectroscopic techniques. Novel concepts for sintering mechanism of γ-Al_2O_3 and the role of La addition to enhance the thermal stability were proposed. La atoms on γ-Al_2O_3 are present in a highly dispersed form when the loading amount is less than 0.2 mmol $g(Al_2O_3)^{-1}$, and form aggregates above this concentration. The isolated La species are stable without structural transformation below 1273 K, but aggregated species change their structure to $LaAlO_3$ perovskite at 1073 K. The addition of La atom to γ-Al_2O_3 poisons strong Lewis acid sites on γ-Al_2O_3, and converts them to new Lewis acid sites with medium strength. The titration of strong Lewis acid sites on Al_2O_3 is the key point to enhance thermal stability of alumina-based catalyst.

Introduction

The transition alumina is one of the most important catalyst materials. The alumina itself, and metal- and/or metal-oxide-promoted ones are utilized for numerous kinds of industrial processes. With increasing temperature, transition alumina decreases the surface area and changes the crystalline phase from γ- through δ-, θ-, and finally to α-phase. The phase transformation to α-phase and decrease of its surface area, so-called sintering, are serious problem for using alumina-based catalysts without deactivation, especially at a high temperature and in the presence of H_2O vapor.[1−4]

The addition of La atom to alumina-based catalyst is commonly performed to enhance thermal stability of the catalyst. There are many studies dealing with states of promoted La and the effects against sintering, and many hypotheses about the effect of La addition have been proposed.[1−3,5−18] Bettman proposed that a two-dimensional La_2O_3 layer on transition alumina decreases the surface energy, resulting in the suppression of sintering.[6] It has been proposed that ionic radii of additives play an important role in enhancing the thermal stability of alumina.[3,8,9,15] On the other hand, surface $LaAlO_3$ phase formed on Al_2O_3 was proposed to improve durability of alumina-based catalyst against high temperature.[3,5,12,18] The formation of a $LaAl_{11}O_{18}$ hexaaluminate phase was also proposed to be a key substance used for catalyst without deactivation at higher temperatures.[10] However, crystalline $LaAlO_3$ was detected at a loading amount above 16%. On the other hand, it has been reported that only a small amount of La doping (ca. 1 mol %) is sufficient for suppression of sintering.[3,7,9,16,19] The XRD characterization is not effective when a crystalline size is less than 100 Å or the concentration is quite low. XPS characterization demonstrated that binding energy of La $3d_{5/2}$ for low loadings is higher than that of $LaAlO_3$.[19,20] It remains unclear whether the perovskite or hexaaluminate phase forms on alumina only at a loading amount less than 10 wt %, and how the addition of La to Al_2O_3 affects the thermal stability.

The γ-Al_2O_3 itself possesses both acid and base sites, and γ-Al_2O_3 itself is widely utilized as industrial dehy-

* Corresponding author. Tsunehiro Tanaka. Fax: +81-75-383-2561. E-mail: tanaka@dcc.mbox.media.kyoto-u.ac.jp.

(1) Arai, H.; Machida, M. *Appl. Catal. A* **1996**, *138*, 161−176.
(2) Burtin, P.; Brunelle, J. P.; Pijiolat, M.; Soustelle, M. *Appl. Catal.* **1987**, *34*, 239−254.
(3) Schaper, H.; Doesburg, E. B. M.; van Reijen, L. L. *Appl. Catal.* **1983**, *7*, 211−220.
(4) Johnson, M. F. L. *J. Catal.* **1990**, *123*, 245−259.
(5) Beguin, B.; Garbowski, E.; Primet, M. *Appl. Catal.* **1991**, *75*, 119−132.
(6) Bettman, M.; Chase, R. E.; Otto, K.; Weber, W. H. *J. Catal.* **1989**, *117*, 447−454.
(7) Chen, X. Y.; Liu, Y.; Niu, G. X.; Yang, Z. X.; Bian, M. Y.; He, A. *Appl. Catal., A* **2001**, *205*, 159−172.
(8) Church, J. S.; Cant, N. W.; Trimm, D. L. *Appl. Catal., A* **1994**, *107*, 267−276.
(9) Loong, C. K.; Richardson, J. W.; Ozawa, M. *J. Alloys Compd.* **1997**, *250*, 356−359.
(10) Matsuda, S.; Kato, A.; Mizumoto, M.; Yamashita, H. *Proc.−Inter. Congr. Catal. 8th* **1984**, 879−889.
(11) Okada, K.; Hattori, A.; Taniguchi, T.; Nukui, A.; Das, R. N. *J. Am. Ceram. Soc.* **2000**, *83*, 928−932.
(12) Oudet, F.; Courtine, P.; Vejux, A. *J. Catal.* **1988**, *114*, 112−120.
(13) Ozawa, M.; Kato, O.; Suzuki, S.; Hattori, Y.; Yamamura, M. *J. Mater. Sci. Lett.* **1996**, *15*, 564−567.
(14) Ozawa, M.; Kimura, M.; Isogai, A. *J. Less-Common Met.* **1990**, *162*, 297−308.
(15) Ozawa, M.; Kimura, M.; Isogai, A. *J. Mater. Sci.* **1991**, *26*, 4818−4822.
(16) Rossignol, S.; Kappenstein, C. *Int. J. Inorg. Mater.* **2001**, *3*, 51−58.
(17) Schaper, H.; Amesz, D. J.; Doesburg, E. B. M.; van Reijen, L. L. *Appl. Catal.* **1984**, *9*, 129−132.
(18) Wachowski, L.; Kirszensztejn, P.; Lopatka, R.; Czajka, B. *Mater. Chem. Phys.* **1994**, *37*, 29−38.
(19) Haack, L. P.; de Vries, J. E.; Otto, K.; Chattha, M. S. *Appl. Catal., A* **1992**, *82*, 199−214.
(20) Haack, L. P.; Peters, C. R.; Devries, J. E.; Otto, K. *Appl. Catal., A* **1992**, *87*, 103−114.

10.1021/cm034732c CCC: $25.00
Published on Web 11/07/2003

dration catalysts.[21−23] On the other hand, aluminas promoted by alkali-metals, alkali-fluorides, alkali-amides, and/or alkali-hydroxide are utilized as super or strong base catalysts.[22,24−31] Lanthanum oxide itself is a typical solid base. Therefore, addition of lanthanum to alumina should change the properties of the catalyst surface. We have confirmed that addition of lanthanoid atom (Ln) to γ-Al_2O_3 poisons both the original base and acid sites of γ-Al_2O_3, and generates new-type Lewis acid site. In a series of Ln/Al_2O_3 catalysts, 0.2−0.5 mmol Yb/Al_2O_3 exhibited the highest activity for α-pinene isomerization.[32]

From these viewpoints, we considered the acid−base properties of La/Al_2O_3 catalysts, and relationships against stabilization effect of La to γ-Al_2O_3. In the present study, we investigated alumina-supported lanthanum oxides to clarify their acid−base property and structures and their structural transformation upon thermal treatment. To examine the local structure around La, we employed La K-edge XAFS instead of the usual La L_{III} edge XAFS.[33] In the case of La, only restricted information can be obtained from L_{III}-edge EXAFS because of the interference by the L_{II}-edge. La L_{III}-edge EXAFS is available for a narrow *k*-range no more than 10 $Å^{-1}$, leading to the lack of contribution from heavy-element (La−La pair) to EXAFS due to their characteristic dependence of backscattering amplitudes upon *k*.[34,35] On the other hand, La K-edge EXAFS could be available without any restrictions. La K-edge EXAFS with a wide *k*-range contains much more information than L_{III}-edge EXAFS.[33]

Experimental Section

Material. La/Al_2O_3 catalyst was prepared by impregnation of γ-Al_2O_3 (JRC-ALO4; 174 $m^2\ g^{-1}$) with an aqueous solution of $La(NO_3)_3{\cdot}xH_2O$ (Nacalai, 99.5%) at 353 K, followed by calcination at 773 K for 5 h.[33] These samples are referred to as *x* mmol La/Al_2O_3 (*x* stands for loading amount of La atom per one gram of Al_2O_3). Further calcination was performed at 873, 1073, and 1273 K for 3 h. The sintered sample was prepared by calcination at 1423 K for 6 h. The surface areas are summarized in Table 1.

Table 1. BET Specific Surface Area of La/Al_2O_3

loading amount			calcined temperature/K				conc.[a]
mmol[b]	wt %[c]	La/Al[d]	873	1073	1273	1423	(atom/nm^2)
0[e]			175	153	117	46	
0.1	1.6	0.005	166	159	118	72	0.36
0.2	3.2	0.010	165	156	132	69	0.73
0.5	7.5	0.025	153	142	107	67	1.97
1.0	14	0.051	137	122	105	52	4.39
2.0	25	0.10	103	89	56	41	11.7
3.4	36	0.17	73	59	34		28.0

[a] La concentrations estimated with surface area of samples calcined at 873 K. [b] Mmol of La per 1 g of Al_2O_3. [c] Wt% as La_2O_3. [d] Atomic ratio. [e] JRC-ALO4 (γ-Al_2O_3) itself.

La_2O_3 was prepared by thermal decomposition of $La(NO_3)_3$ at 1273 K for 5 h. $LaAlO_3$ (perovskite, denoted as *P*) and $LaAl_{11}O_{18}$ (hexaaluminate, denoted as *HA*) were synthesized by a citric acid process. A mixture of lanthanum nitrate (5 mmol for *P*; 2 mmol for *HA*), aluminum nitrate (5 mmol for *P*; 22 mmol for *HA*), and citric acid (50 mmol) was dissolved at 348 K in 2 mL of distilled water. The solution was stirred vigorously until it was solidified, followed by aging at 383 K for 48 h. The formed amber foam was precalcined at 623 K for 2 h, followed by calcination at 1273 K (*P*) or 1673 K (*HA*) for 5 h. After calcination, it was quenched to room temperature. II-$La_2O_2CO_3$ was synthesized by calcination of $La_2(CO_3)_3{\cdot}8H_2O$ (Wako, 99.5%) under 30 kPa of dry CO_2 at 973 K for 6 h. The δ- and α-Al_2O_3 were prepared by calcination of γ-Al_2O_3 in the air for 6 h at 1273 and 1573 K, respectively.

Catalysis. The α-pinene isomerization was carried out under dry N_2 atm using a stirred batch reactor at 323 K.[36,37] The 2-butanol decomposition was carried out with a closed circulation system (dead volume, 200 cm^3) at 423 K.[32] Before each reaction, a sample was evacuated at 1073 K for 0.5 h and calcined under 6.66 kPa of O_2 for 1 h, followed by evacuation at the same temperature for 1 h. In an experiment for α-pinene isomerization, the reactor was loaded with 2 mL (12.6 mmol) of α-pinene (Nacalai, EP, 99.8%) and 50 mg of catalyst. In an experiment for 2-butanol decomposition, 150 μmol of 2-butanol was diluted with 300 μmol of dry N_2. Products were analyzed by FID gas chromatograph (Shimadzu).

Characterization. The BET specific surface area measurement was carried out with BELSORP 28SA (BEL Japan) using a N_2 adsorption isotherm at 77 K. Prior to a measurement, each sample was outgassed at 673 K for 3 h.

X-ray diffraction patterns of samples were obtained with a Rigaku Geigerflux diffractometer using Ni-filtered Cu Kα radiation (λ averaged as 1.5418 Å).

FTIR spectra of adsorbed pyridine were recorded using a Perkin-Elmer Paragon 1000 spectrometer with the resolution of 4 cm^{-1}. The 30-mg sample (40 mg for La_2O_3) was pressed into a self-supporting wafer (20 mm diam.), and was mounted in an in situ IR cell equipped with BaF_2 windows. A wafer was pretreated in the same way as for the catalytic reaction. The pretreated wafer was exposed to 1.0 kPa of pyridine vapor at 423 K for 5

(21) Pines, H.; Manassen, J. *Adv. Catal.* **1966**, *16*, 49−93.
(22) Tanabe, K.; Holderich, W. F. *Appl. Catal., A* **1999**, *181*, 399−434.
(23) Tanabe, K.; Misono, M.; Ono, Y.; Hattori, H. In *New Solid Acids and Bases*; Kodansha: Tokyo, 1989; pp 78−91.
(24) Ando, T. In *Acid−Base Catalysis II*; Hattori, H., Misono, M., Ono, Y., Eds.; Kodansha: Tokyo, 1993; pp 9−20.
(25) Baba, T. *Catal. Surv. Jpn.* **2000**, *4*, 17−29.
(26) Kabashima, H.; Tsuji, H.; Nakata, S.; Tanaka, Y.; Hattori, H. *Appl. Catal., A* **2000**, *194*, 227−240.
(27) Suzukamo, G.; Fukao, M.; Hibi, T.; Tanaka, K.; Minobe, M. *Stud. Surf. Sci. Catal.* **1997**, *108*, 649−656.
(28) Suzukamo, G.; Fukao, M.; Minobe, M. *Chem. Lett.* **1987**, 585−588.
(29) Yamaguchi, T.; Zhu, J. H.; Wang, Y.; Komatsu, M.; Ookawa, M. *Chem. Lett.* **1997**, 989−990.
(30) Kijenski, J.; Marczewski, M.; Malinowski, S. *React. Kinet. Catal. Lett.* **1977**, *7*, 151.
(31) Kijenski, J.; Marczewski, M.; Malinowski, S. *React. Kinet. Catal. Lett.* **1977**, *7*, 157.
(32) Yamamoto, T.; Tanaka, T.; Matsuyama, T.; Funabiki, T.; Yoshida, S. *J. Phys. Chem. B* **2001**, *105*, 1908−1916.
(33) Yamamoto, T.; Tanaka, T.; Matsuyama, T.; Funabiki, T.; Yoshida, S. *J. Synchrotron Radiat.* **2001**, *8*, 634−636.
(34) Teo, B. K.; Lee, P. A. *J. Am. Chem. Soc.* **1979**, *101*, 2815−2832.
(35) Teo, B. K. *EXAFS: Basic Principles and Data Analysis*; Springer-Verlag: Berlin, 1986.
(36) Yamamoto, T.; Matsuyama, T.; Tanaka, T.; Funabiki, T.; Yoshida, S. *Phys. Chem. Chem. Phys.* **1999**, *1*, 2841−2849.
(37) Yamamoto, T.; Tanaka, T.; Funabiki, T.; Yoshida, S. *J. Phys. Chem. B* **1998**, *102*, 5830−5839.

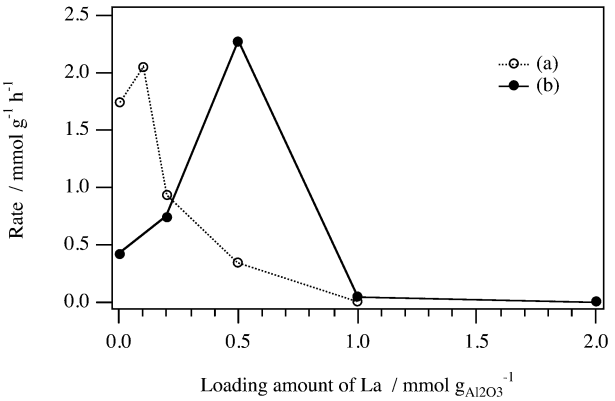

Figure 1. Results of 2-butanol decomposition at 423 K (a) and α-pinene isomerization at 323 K (b).

min, followed by evacuation at the same temperature for 1 h. After the samples cooled to room temperature, each spectrum was recorded in a transmission mode.

X-ray absorption experiments were carried out on the BL01B1 at SPring-8 (Hyogo, Japan).[38] The ring energy was 8 GeV, and the stored current was 70−100 mA. The La K-edge X-ray absorption spectra were recorded in a transmission mode at room temperature using a Si(311) two-crystal monochromator. Higher harmonics were eliminated with 1.2 mrad Rh-coated mirrors. The dispersive X-ray was collimated to be a parallel ray by a total reflection mirror, at an upper stream 32.9 m from an X-ray source. The height of the X-ray size was 1.0 mm. The energy was calibrated by a top of white line of $LaAlO_3$ (38950 eV) and the calibration experiment was performed after every five measurements. Energy steps of measurements in XANES and EXAFS regions were 1 and 4 eV, respectively. Data reduction was performed using a FACOM M1800 computer in the Kyoto University Data Processing Center. The normalization method has been previously reported in detail.[39] The Fourier transform was performed on EXAFS in the k range of ca. 3.2−14 $Å^{-1}$. For curve-fitting analysis, the backscattering amplitude and phase shift functions of La−O pair were obtained from a k^3-weighted EXAFS spectrum of $La(OH)_3$ (coordination number 9, interatomic distance 2.577 Å).[40]

Results and Discussion

(1) Acid Base Property. *Catalysis.* Figure 1 shows initial rates for 2-butanol decomposition and α-pinene isomerization. The catalytic performance depended on the loading amounts of La. In the case of α-pinene isomerization, the maximum activity was observed over 0.5 mmol $g(Al_2O_3)^{-1}$. The fact that La_2O_3 and γ-Al_2O_3 themselves were inert at the reaction condition indicates that active species was generated on the catalyst surface of Al_2O_3 by addition of La. The main products were camphene (50%) and limonene (30%), and the amount of produced β-pinene was scarce. The α-pinene isomerization is one of the excellent test reactions for acid−base catalyst. Over a solid base catalyst, only equilibrium reaction between α-pinene and β-pinene proceeds. In contrast, various kinds of bicyclic and monocyclic species are produced over acid catalysts, and the selectivities depend on the maximum acid strength.[37,41−45] These selectivities obtained in the present study show that all the La/Al_2O_3 acted as solid acid, and the acid strengts are similar to each other. No polymerized products were observed, indicating that the maximum acid strength of La/Al_2O_3 is not very strong ($+3.3 \le H_0 < -5.6$, H_0; Hammett acidity function).

Table 2. Product Distributions of 2-Butanol Decomposition[a]

		selectivity[c]		
catalyst	T (K)[b]	MEK[d]	but-1-ene	but-2-enes
γ-Al_2O_3	423	0	30	70
0.1 mmol La/Al_2O_3	423	0	23	77
0.2 mmol La/Al_2O_3	423	0	28	72
0.5 mmol La/Al_2O_3	423	0	30	70
La_2O_3	523	14	82	4

[a] Catalyst 50 mg; 2-butanol 150 μmol. [b] Reacted temperature. [c] At 20% conversion. [d] Methyl ethyl ketone.

As is well-known, γ-Al_2O_3 itself exhibited a high activity of 2-butanol dehydration.[21,22,46] The addition of La atom (0.1 mmol $g(Al_2O_3)^{-1}$) slightly raised the activity. But further addition decreased the activity, and became zero when it was 1.0 mmol $g(Al_2O_3)^{-1}$. This phenomenon is the same as the case of Yb/Al_2O_3 system.[32] Addition of lanthanum increased a yield of but-1-ene, but did not change amounts of produced but-2-enes. This shows that an active site for but-2-ene production forms by addition of La to alumina, but further addition covered the active sites. A difference in the activity between γ-Al_2O_3 and 0.1 mmol La/Al_2O_3 was not remarkable; however, a difference in the amount of each product was noticeable. Decomposition of a secondary alcohol gives three kinds of products. In general, acid sites catalyze dehydration with Saytzeff orientation leading to the production of internal olefins, and base sites catalyze dehydrogenation leading to the ketones, and acid−base pair sites catalyze dehydration with Hoffman orientation (E1cB mechanism) leading to terminal olefins.[46−50] As discussed in our previous paper, selectivity for but-1-ene over typical solid acid is about 15%, and coexistence of basic site with acid site increases the selectivity.[32] The obtained selectivities at a 20% conversion are listed in Table 2. The selectivity toward but-1-ene was about 30% for both γ-Al_2O_3 and

(38) Uruga, T.; Tanida, H.; Yoneda, Y.; Takeshita, K.; Emura, S.; Takahashi, M.; Harada, M.; Nishihata, Y.; Kubozono, Y.; Tanaka, T.; Yamamoto, T.; Maeda, H.; Kamishima, O.; Takabayashi, Y.; Nakata, Y.; Kimura, H.; Goto, S.; Ishikawa, T. *J. Synchrotron Radiat.* **1999**, *6*, 143−145.
(39) Tanaka, T.; Yamashita, H.; Tsuchitani, R.; Funabiki, T.; Yoshida, S. *J. Chem. Soc., Faraday Trans. 1* **1988**, *84*, 2987−2999.
(40) Ali, F.; Chadwick, A. V.; Smith, M. E. *J. Mater. Chem.* **1997**, *7*, 285−291.
(41) Corma, A.; Garcia, H. *Catal. Today* **1997**, *38*, 257−308.
(42) Ohnishi, R.; Tanabe, K. *Chem. Lett.* **1974**, 207−210.
(43) Ohnishi, R.; Tanabe, K.; Morikawa, S.; Nishizaki, T. *Bull. Chem. Soc. Jpn.* **1974**, *47*, 571−574.
(44) Stanislaus, A.; Yeddanapalli, L. M. *Can. J. Chem.* **1972**, *50*, 61−74.
(45) Tanabe, K. In *Solid Acids and Bases*; Kodansha: Tokyo, 1970; pp 119−125.
(46) Tanabe, K.; Misono, M.; Ono, Y.; Hattori, H. In *New Solid Acids and Bases*; Kodansha: Tokyo, 1989; pp 260−267.
(47) Auroux, A.; Artizzu, P.; Ferino, I.; Monaci, R.; Rombi, E.; Solinas, V.; Petrini, G. *J. Chem. Soc., Faraday Trans.* **1996**, *92*, 2619−2624.
(48) Auroux, A.; Artizzu, P.; Ferino, I.; Solinas, V.; Leofanti, G.; Padovan, M.; Messina, G.; Mansani, R. *J. Chem. Soc., Faraday Trans.* **1995**, *91*, 3263−3267.
(49) Thomke, K. *Proc. Int. Congr. Catal. 6th* **1977**, *I*, 303−315.
(50) Yamaguchi, T.; Tanabe, K. *Bull. Chem. Soc. Jpn* **1974**, *47*, 424−429.

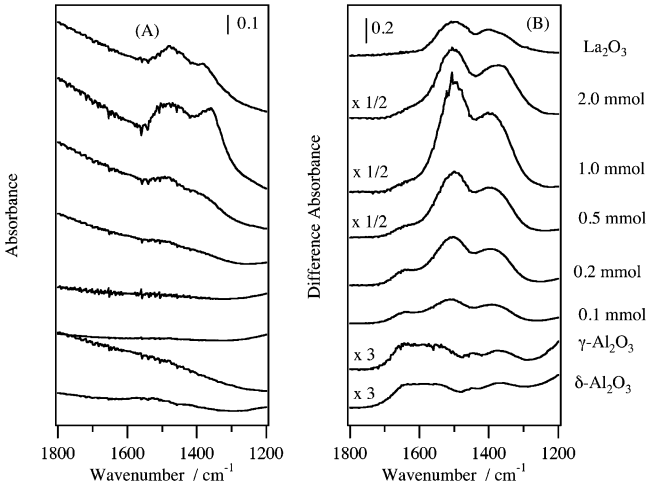

Figure 2. FTIR spectra of La_2O_3, La/Al_2O_3, and γ- and δ-Al_2O_3: evacuated at 773 K (A), and difference spectra of those evacuated between ones evacuated at 773 K and room temperature (B).

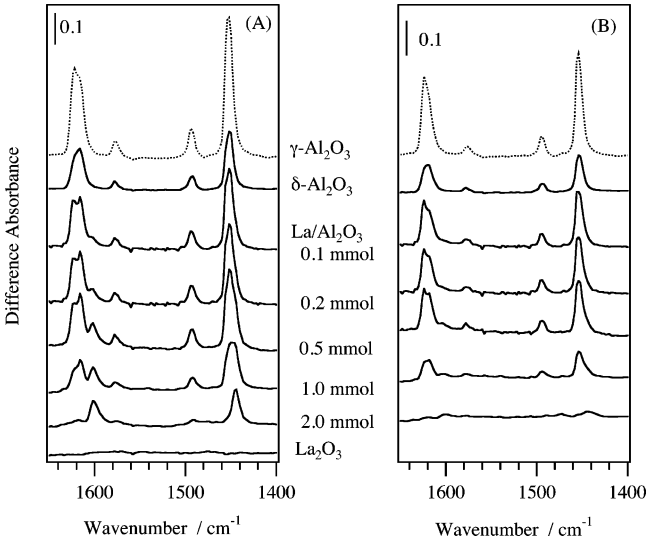

Figure 3. FTIR spectra of adsorbed pyridine at 423 K (A) and 473 K (B).

La/Al_2O_3. This shows that some base sites exist on the catalyst surfaces, but the amounts are much less than those of acid sites. La_2O_3 itself was inert at 423 K, but active at 523 K. Rare earth oxide is known as a typical solid base; however, it possesses Lewis acid sites as well. Therefore, La_2O_3 produced but-1-ene of E1cB orientation mainly accompanied by methyl ethyl ketone of dehydrogenates.

IR Spectra. Because La/Al_2O_3 catalyst samples are stored in the air, much CO_2 and H_2O are adsorbed on the catalyst surface. To evaluate the basic properties of a catalyst surface, we utilized IR spectra of adsorbed CO_2 species. We measured two kinds of spectra: one is a spectrum of the sample evacuated at room temperature for 1 h (spectrum *I*); another is that of a sample pretreated at 773 K (spectrum *II*). A carbonate species retained on spectrum *II* corresponds to a strong basic site. Figure 2 (A) shows IR spectra treated at 773 K. No CO_2-related species were observed when the loading amount was less than 0.5 mmol La g$(Al_2O_3)^{-1}$. Above that loading amount, two bands appeared around 1360 and 1480 cm^{-1}. The spectrum of La_2O_3 exhibited a pair of bands at 1378 and 1478 cm^{-1}. These two bands are assigned to symmetric and anti-symmetric vibration modes of monodentate carbonate species, respectively.[51] This shows that strong basic sites generated on La/Al_2O_3 when the loading amount was above 1.0 mmol g$(Al_2O_3)^{-1}$. The amounts of strong base sites for La/Al_2O_3 were more than that of La_2O_3. This might be due to differences of the surface area.

Difference spectra between spectra *I* and *II* reflect on the whole basic property of a catalyst. Figure 2 (B) shows the difference IR spectra of adsorbed CO_2 species. Spectra of δ- and γ-Al_2O_3 gave absorption bands assigned to bicarbonate species (1445 and 1650 cm^{-1}) accompanied by monodentate carbonate species.[51,52] These two spectra are identical to each other, indicating that basic properties of the two aluminas are quite similar to each other. Addition of La to γ-Al_2O_3 increased band intensities, which were due to monodentate carbonate species (1390 and 1510 cm^{-1}). This shows that addition of La to Al_2O_3 generates basic sites on the surface. The amount of basic sites reached a maximum at the loading amount of 1.0 mmol g$(Al_2O_3)^{-1}$, but the strength was not so strong that majority of carbonates was desorbed below 773 K. The strong basic sites appeared on a catalyst surface when the loading amount was above 2.0 mmol g$(Al_2O_3)^{-1}$. Of course, the base amount for 2.0 mmol La/Al_2O_3 was slightly underestimated because some carbonate species still existed on the Spectrum *II*. Decrease of basic sites relates to their apparent surface area of La-related sites.

Figure 3 shows IR spectra of adsorbed pyridine at 423 K. A spectrum on γ-Al_2O_3 exhibited four bands (1450, 1492, 1578, and 1620 cm^{-1}) which correspond to pyridine species adsorbed on Lewis acid sites (L-pyridine).[32,52] On the other hand, La/Al_2O_3 gave two kinds of 8a mode L-pyridine at 1620 and 1604 cm^{-1}. With increasing loading amounts, a band intensity at 1620 cm^{-1} went on decreasing and another band grew around 1608 cm^{-1}. It should be noted that intensity of the band at 1620 cm^{-1} on La/Al_2O_3 was smaller than that of γ-Al_2O_3 itself, but a sum of two band areas of 8a-mode L-pyridine on La/Al_2O_3 was almost the same as that on γ-Al_2O_3. Then, we conclude that addition of La atom to γ-Al_2O_3 converts original Lewis acid sites on γ-Al_2O_3 to another kind of Lewis acid sites. There were no bands around 1540 cm^{-1}, which is characteristic to pyridine species on strong Brønsted acid sites. It should be noted that this does not imply the absence of weak Brønsted acid sites which could not transfer the proton to pyridine.[52,53] Because a large amount of the acid sites on La/Al_2O_3 were Lewis acid sites, we did not investigate the weak Brønsted acid sites. To examine the strength of acid sites, we collected IR spectra of evacuated pyridine-adsorbed sample at higher temperature. Figure 3 (B) shows IR spectra of adsorbed pyridine after evacuation at 473 K. Almost all the bands around 1600 cm^{-1} disappeared, although the bands around 1620 cm^{-1} remained unchanged; clearly showing that the acid

(51) Little, L. H.; Kiselev, A. V.; Lygin, V. I. *Infrared Spectra of Adsorbed Species*; Academic Press: London, 1966.
(52) Morterra, C.; Magnacca, G. *Catal. Today* **1996**, *27*, 497−532.
(53) Buzzoni, R.; Bordiga, S.; Ricchiardi, G.; Lamberti, C.; Zecchina, A.; Bellussi, G. *Langmuir* **1996**, *12*, 930−940.

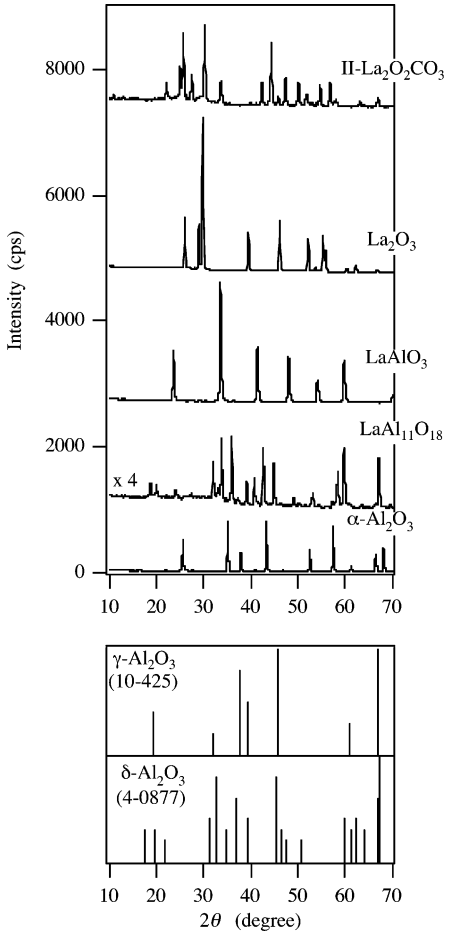

Figure 4. Cu Kα XRD patterns of reference compounds and JCPDS files.

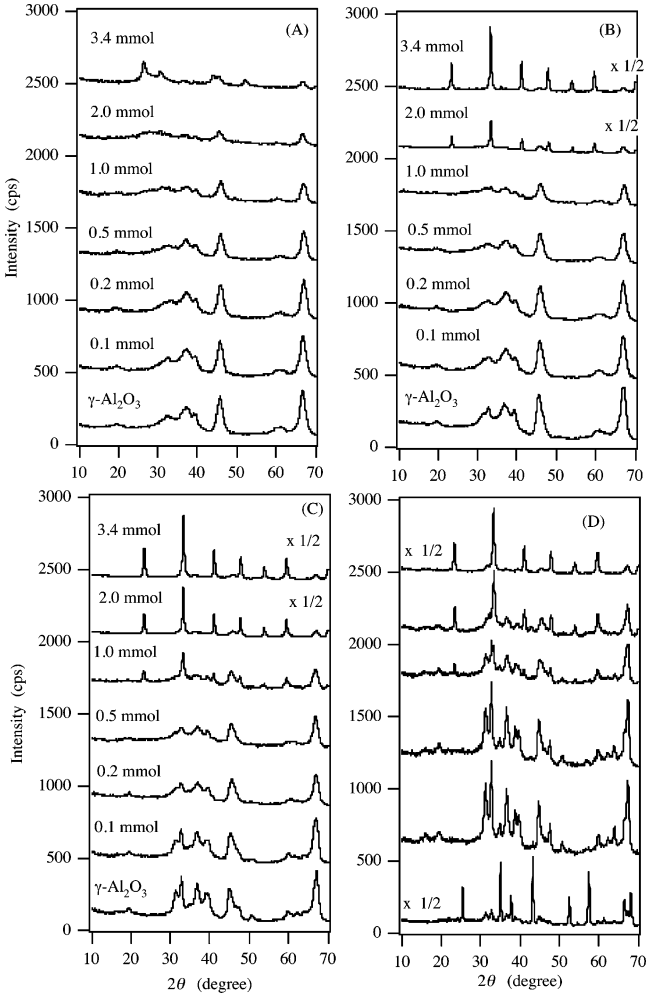

Figure 5. Cu Kα XRD patterns of La/Al_2O_3 catalyst calcined at 873 (A), 1073 (B), 1273 (C), and 1423 K (D).

strengths of La-related acid sites were weaker than that of γ-Al_2O_3 itself. The difference in frequency of the same 8a mode of pyridine relates to degree of perturbation from acid sites. The acidity strength of an adsorption site affects the shift of the pyridine bands.[52−54] The lower wavenumber of generated 8a mode of Lewis pyridine (1608 cm^{-1}) comparing to the original one (1620 cm^{-1}) also demonstrates the order of acid strength of Lewis acid site on La/Al_2O_3. The IR spectrum of δ-Al_2O_3 gave similar bands to that of γ-Al_2O_3. The wavenumbers of 8a mode of Lewis pyridine were identical to each other, indicating that the acid strengths were not so differed between δ-Al_2O_3 and γ-Al_2O_3. The difference in intensities reflects on the amount of acid sites between them. It shows that acidity of δ-Al_2O_3 is higher than those of La-related acid sites.

(2) Structural Characterization. *XRD.* Figure 4 shows XRD patterns of reference compounds and JCPDS files, and Figure 5 shows XRD patterns of La/Al_2O_3 catalyst calcined at different temperatures. At a calcination temperature of 873 K, all patterns except for 3.4 mmol La/Al_2O_3 exhibited typical peaks assigned to γ-Al_2O_3 only. Additional peaks appeared on 3.4 mmol La/Al_2O_3, but they were missing in any JCPDS files. The decomposition temperature of $La_2O_2CO_3$ to La_2O_3 is 1020 K.[55] Therefore, the peaks might be due to an intermediate phase between La_2O_3 and $La_2O_2CO_3$, which was formed at the catalyst preparation step. This is supported by the IR characterization which showed that the bands due to carbonate species were kept in the spectra of $La_2O_2CO_3$ and $La_2(CO_3)_3$ evacuated below 877 K.[56,57] At a calcination temperature of 1073 K, formation of $LaAlO_3$ perovskite was confirmed on La/Al_2O_3, the loading amount of which was higher than 2.0 mmol $g(Al_2O_3)^{-1}$. Lanthanum species on 1.0 mmol La/Al_2O_3 was crystallized to $LaAlO_3$ at 1273 K. In the cases of 0.1 mmol La/Al_2O_3 and γ-Al_2O_3 support itself, γ-Al_2O_3 was transformed to δ-phase after thermal treatment at 1273 K. At the calcination temperature of 1373 K, α-Al_2O_3 formed in the absence of La. When La/Al_2O_3 was calcined at 1373 K, crystalline $LaAlO_3$ was confirmed at the La concentration above 0.5 mmol $g(Al_2O_3)^{-1}$. Below the La loadings, the $LaAlO_3$ phase was not detected by XRD analysis, regardless of the calcination temperature. On the other hand, only δ-Al_2O_3 phase was detected on 0.1 and 0.2 mmol La/Al_2O_3 clearly showing that addition of La suppresses a phase transformation of Al_2O_3 from δ- to α-phase, but the excess addition causes the $LaAlO_3$ perovskite formation

(54) Bonino, F.; Damin, A.; Bordiga, S.; Lamberti, C.; Zecchina, A. *Langmuir* **2003**, *19*, 2155−2161.

(55) Squir, G. D.; Luc, H.; Puxley, D. C. *Appl. Catal. A* **1994**, *108*, 261−278.

(56) Levan, T.; Che, M.; Tatibouet, J. M.; Kermarec, M. *J. Catal.* **1993**, *142*, 18−26.

(57) Taylor, R. P.; Schrader, G. L. *Ind. Eng. Chem. Res.* **1991**, *30*, 1016−1023.

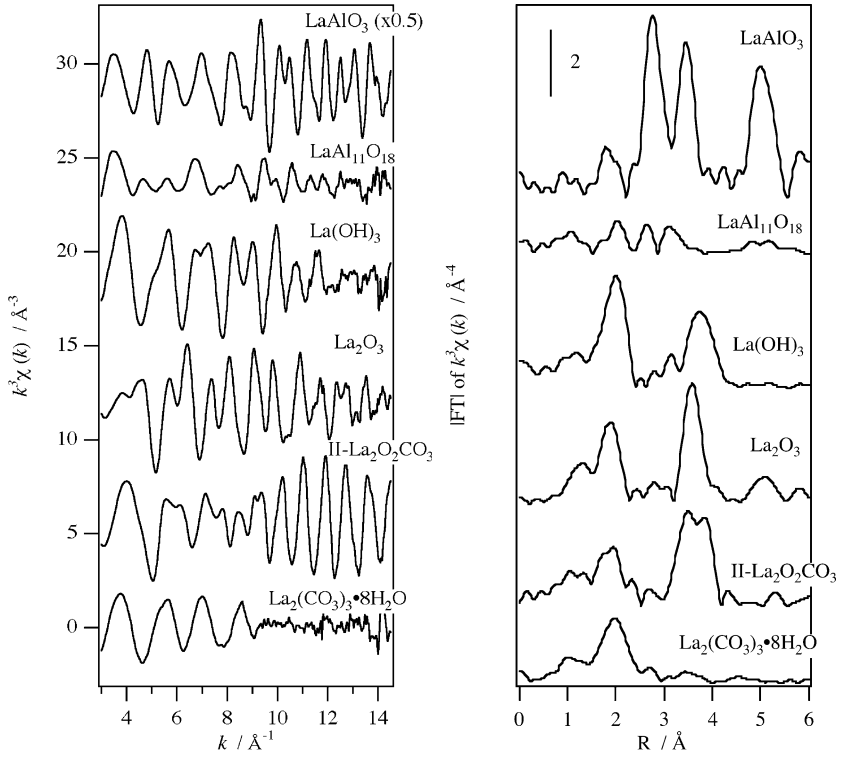

Figure 6. La K-edge k^3-weighted EXAFS spectra of reference compounds and their Fourier transforms.

easily. Crystalline $LaAl_{11}O_{18}$ phase was not detected on any of the XRD patterns.

EXAFS. Figure 6 shows La K-edge EXAFS spectra and their Fourier transforms of reference compounds. $LaAlO_3$ gives strong EXAFS oscillation and radial structure function (RSF), whereas those of $LaAl_{11}O_{18}$ are much weaker. $LaAlO_3$ has a perovskite structure with cubic symmetry, and the first coordination sphere around La consists of twelve oxygen atoms of the same distance.[58] Nevertheless, the first peak of $LaAlO_3$ in the RSF at K-edge is very tiny. In RSFs of $La(OH)_3$, La_2O_3, and II-$La_2O_2CO_3$, strong peaks appear around 2.0 and 3.5 Å due to La−O and La−(O)−La contributions, respectively. An EXAFS spectrum of $La_2(CO_3)_3{\cdot}8H_2O$ does not have any oscillations above 10 $Å^{-1}$ and gives no peaks above 3 Å in the RSF, indicating that little La−La contributions exist on $La_2(CO_3)_3{\cdot}8H_2O$.

Figure 7 shows La K-edge EXAFS spectra of fresh La/Al_2O_3 and their Fourier transforms. These catalysts were calcined at 773 K, and were stored in the air. As a result, much H_2O and CO_2 was adsorbed onto the catalyst surface. When the loading amounts were less than 1.0 mmol La $g(Al_2O_3)^{-1}$, the EXAFS oscillation amplitude decreased monotonically with k and little oscillation was observed in the k-region higher than 10 $Å^{-1}$. Their RSFs give a single peak around 2 Å, and do not have any peaks above 3 Å, showing that La−La contributions do not exist. These EXAFS spectra and RSFs are similar to those of $La_2(CO_3)_3{\cdot}8H_2O$. On the other hand, distinct oscillation was observed up to 14 $Å^{-1}$ when loading amount was above 2.0 mmol La $g(Al_2O_3)^{-1}$, indicating that some La−La contribution exists. The peak height around 2 Å on the RSF was lower than those of lower loadings. Evidently, a part of La species of higher loading catalyst is not uniform and consists of some phases.

Figure 8 shows La K-edge EXAFS spectra and their Fourier transforms of La/Al_2O_3 calcined at 873 K. The present samples were evacuated at the same temperature, and XAFS spectra were collected without exposure to the air. In all RSFs, two peaks are found at around 1.2 and 1.9 Å. The peak at 1.9 Å is due to La−O bond, and the rest is a side lobe of La−O due to nonlinearity of their phase shifts. All the signal intensities were much weaker than those of samples under air. The oscillation amplitude decreased rapidly with k, and little oscillation appeared in the k-region above 9 $Å^{-1}$, indicating that La species are supported on Al_2O_3 in a highly dispersed form and that no La−(O)−La contribution exists. The remarkable decay of the oscillation amplitude should be noted. Decrease in coordination number is one of the reasons for the reduction of the amplitude of EXAFS spectrum. Another reason is due to an extremely large apparent Debye−Waller factor, i.e., surface La species (LaO_x) have many kinds of La−O bond-lengths, and/or the symmetry of LaO_x polyhedra on Al_2O_3 is quite distorted. Existence of some La−O bonds with different lengths might cause counteracting of the EXAFS oscillations. The irregular frequencies of EXAFS oscillation support this deduction.

Figure 9 shows La K-edge EXAFS spectra and their Fourier transforms of La/Al_2O_3 calcined at 1273 K. These spectra were recorded without exposure to the air as well. Although spectra of 0.1 and 0.2 mmol La/Al_2O_3 exhibited spectra identical to those calcined at 873 K, spectra of higher loadings above 1.0 mmol $g(Al_2O_3)^{-1}$ were similar to that of $LaAlO_3$ perovskite. In their RSFs, La−Al and La−La contributions were observed at around 2.8 and 3.4 Å, respectively, showing that La species on Al_2O_3 form $LaAlO_3$ at 1273 K when the

(58) Wyckoff, R. W. G. In *Crystal Structures*, 2nd ed.; Interscience Publishers: New York, 1986; Vol. 2, pp 390−402.

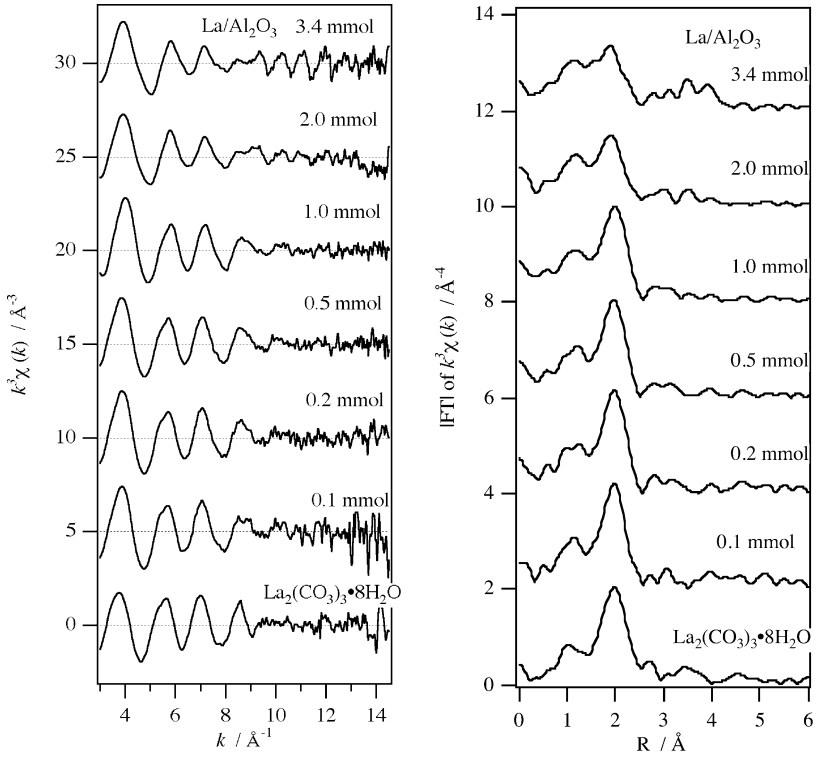

Figure 7. La K-edge k^3-weighted EXAFS spectra of La/Al_2O_3 calcined at 773 K and their Fourier transforms.

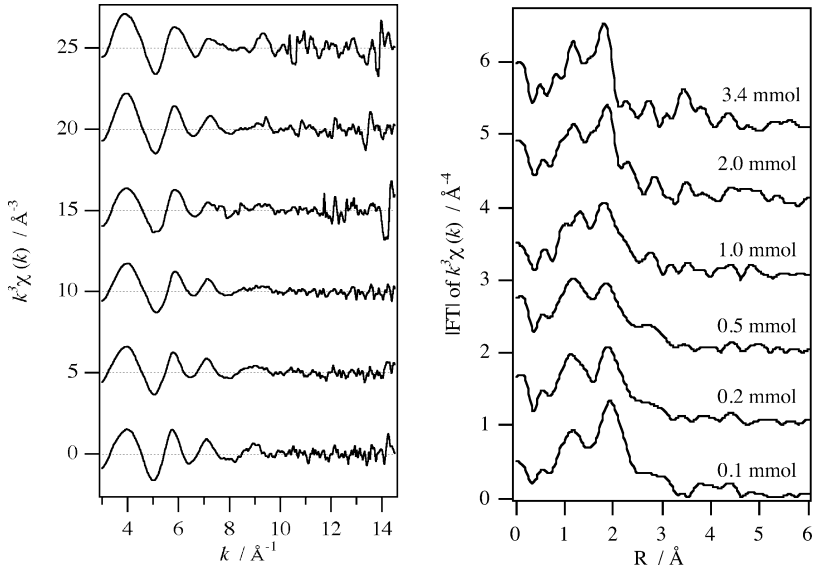

Figure 8. La K-edge k^3-weighted EXAFS spectra of La/Al_2O_3 calcined at 873 K and their Fourier transforms.

loadings were above 1.0 mmol $g(Al_2O_3)^{-1}$. $LaAlO_3$ phase on 0.5 mmol La/Al_2O_3 calcined at 1273 K was not detected by XRD analysis; however, the RSF gave small but distinct peaks due to characteristic La−Al and La−La bonds due to $LaAlO_3$. This reflects that small amounts of La species exist as $LaAlO_3$, and large parts of residual species exist in a highly dispersed form and/or amorphous state.

Curve-Fitting Analysis. To examine local structure around La on La/Al_2O_3 in more detail, we tried a curve-fitting analysis. First we must note that obtained EXAFS parameters of the present curve-fitting analysis for La−O bonding do not always reflect the true coordination sphere. In La_2O_3, the number of the nearest oxygen neighbors of La^{3+} are 3 at 2.38, 1 at 2.45, and 3 at 2.72 Å.[59] Nevertheless, the longer La−O bonding could not be detected as shown in Table 3. It is well-known that La_2O_3 easily reacts with H_2O and/or CO_2 to form hydroxide and/or carbonate even at room temperature. In fact, an EXAFS spectrum of La_2O_3 was strongly affected by H_2O and/or CO_2 contained in the air.[60] Prior to the present XAFS measurement, however, we calcined La_2O_3 at 1273 K under 6.67 kPa of dry O_2 for 3 h again, and put it in a polyethylene bag under dry N_2 without exposure to the air. Therefore, it is impossible that the present La_2O_3 sample had trans-

(59) Wells, A. F. In *Structural Inorganic Chemistry*, 5th ed.; Oxford University Press: New York, 1984; p 546.

(60) Malet, P.; Capitan, M. J.; Centeno, M. A.; Odriozola, J. A.; Carrizosa, I. *J. Chem. Soc.-Faraday Trans.* **1994**, *90*, 2783−2790.

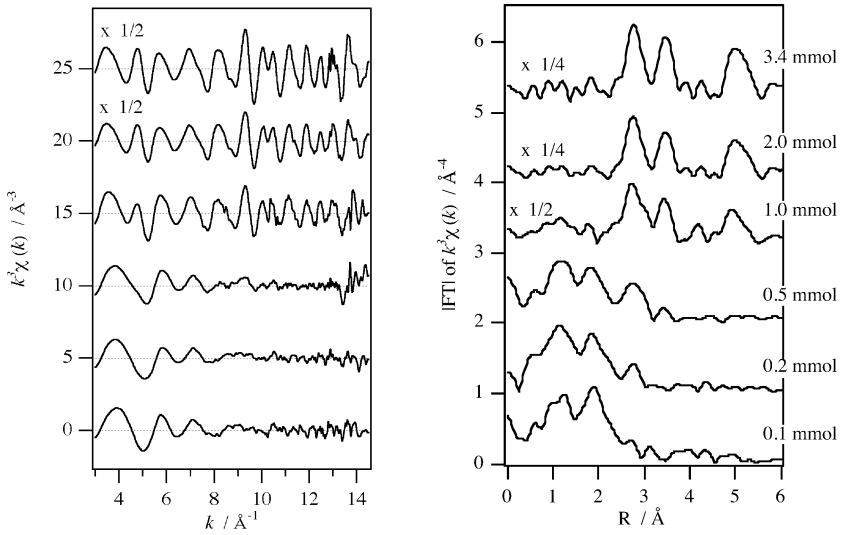

Figure 9. La K-edge k^3-weighted EXAFS spectra of La/Al_2O_3 calcined at 1273 K and their Fourier transforms.

Table 3. Results of Curve-Fitting Analysis for La/Al_2O_3[a]

sample	CN[b]	r/Å[c]	$\Delta\sigma^2$/1000 Å^2 [d]	R (%)[e]
La_2O_3	3.5 ± 0.1	2.41 ± 0.00	−3.2 ± 0.2	16.4[f]
	3.0 ± 6.9	2.75 ± 0.06	56.0 ± 60.6	
	(3.4 ± 0.1	2.40 ± 0.00	−3.3 ± 0.2	14.6)[g]
II-$La_2O_2CO_3$	3.3 ± 0.9	2.45 ± 0.02	−3.0 ± 1.0	13.2
	3.4 ± 0.9	2.61 ± 0.03	−1.2 ± 2.1	
	(6.8 ± 0.2	2.48 ± 0.00	5.3 ± 0.4	20.0)[g]
$La_2(CO_3)_3{\cdot}8H_2O$	7.6 ± 0.1	2.58 ± 0.00	2.9 ± 0.2	11.2
La/Al_2O_3 calcined at 773 K (ex situ)				
0.1 mmol	7.4 ± 0.1	2.56 ± 0.00	3.6 ± 0.2	7.7
0.2 mmol	7.5 ± 0.1	2.57 ± 0.00	3.9 ± 0.1	6.2
0.5 mmol	6.7 ± 0.1	2.56 ± 0.00	3.2 ± 0.1	5.6
1.0 mmol	6.7 ± 0.1	2.56 ± 0.00	4.1 ± 0.1	7.5
2.0 mmol	6.1 ± 0.1	2.52 ± 0.00	6.8 ± 0.2	9.6
3.4 mmol	6.8 ± 0.2	2.50 ± 0.00	9.9 ± 0.4	14.5
La/Al_2O_3 calcined at 873 K (in situ)				
0.1 mmol	4.4 ± 0.1	2.53 ± 0.00	4.0 ± 0.2	8.1
0.2 mmol	4.2 ± 0.1	2.53 ± 0.00	6.3 ± 0.3	10.8
0.5 mmol	4.1 ± 0.1	2.49 ± 0.00	8.0 ± 0.3	13.8
1.0 mmol	4.1 ± 0.2	2.48 ± 0.00	6.7 ± 0.7	27.1
La/Al_2O_3 calcined at 1273 K (in situ)				
0.1 mmol	4.7 ± 0.1	2.53 ± 0.00	7.1 ± 0.3	12.8
0.2 mmol	3.5 ± 0.1	2.52 ± 0.00	7.5 ± 0.4	14.3

[a] Inverse-Fourier range, ΔR = 1.4−2.5 Å; fitting range, Δk = 4.0−12.0 Å^{-1}. [b] Coordination number. [c] Interatomic distance. [d] Relative Debye−Waller factor against that of reference compound ($La(OH)_3$). [e] $e\sqrt{\Sigma(k^3\chi_{\text{experimental}} - k^3\chi_{\text{calculated}})^2/\Sigma(k^3\chi_{\text{experimental}})^2} \times 100$ [f] Inverse-Fourier range, ΔR = 1.4−2.7 Å. [g] Single-shell fitting.

formed to another compound. La L_{III} edge EXAFS characterization for La_2O_3 could confirm the longer La−O contribution with small Debye−Waller factor,[40,60,61] in contrast to the present unrealistic large value for La K-edge. As revealed in our previous paper, contribution of the La−O pair in $LaAlO_3$ perovskite (coordination number 12; interatomic distance 2.671 Å) was quite tiny for La K-edge, but distinct for La L_{III} edge.[33] In fact, RSFs of La/Al_2O_3 calcined at 1273 K did not gave any peaks below 2 Å when the loading amount was above 1.0 mmol $g(Al_2O_3)^{-1}$: note that $LaAlO_3$ perovskite had formed on the catalyst surface. It might show that long La−O bonding (above 2.65 Å) exhibits only a little EXAFS oscillation at La K-edge. The average of La−O bonds in $La_2(CO_3)_3{\cdot}8H_2O$ is 2.61 Å (2.52−2.74 Å, coordination number 10).[62] On the other hand, the estimated parameters were similar to those without the longest 2 La−O bonds (2.575 Å, coordination number 8). We do not know whether this phenomenon is an intrinsic problem at La K-edge.

Table 3 shows a curve fitting analysis of reference compounds and La/Al_2O_3. Under exposure to the air, obtained EXAFS parameters were similar to those of $La_2(CO_3)_3{\cdot}8H_2O$ and $La(OH)_3$ (reference compound) when the loading amounts were less than 2.0 mmol $g(Al_2O_3)^{-1}$. Above that loading amount, the bond length of La−O decreased from 2.56 to 2.50 Å. We suppose that bond lengths of the aggregated species are shorter than those of lanthanum salts such as $La(OH)_3$, which is supported by the result that evaluated bond lengths of La_2O_3 and II-$La_2O_2CO_3$ are 2.40 and 2.48 Å, respectively. After calcination at 873 K, all of the estimated coordination numbers and bond lengths decreased. We note that higher loading of catalyst more than 1.0 mmol $g(Al_2O_3)^{-1}$ could not give adequate fit due to the existence of various kinds of La species and La−O bonding. We have tried two-shell fitting; however, we could not obtain satisfactory fits.

XANES. The phase transformation of supported lanthanum species upon thermal treatment can be confirmed by XANES spectra clearly and quantitatively. Figure 10 shows La−K edge XANES spectra of reference compounds. Despite the broad natural width of La K-edge (Γ = 14.1 Å),[63] each XANES spectrum of a reference compound is distinguishable and gives different top energy of the white line.

Figure 11 shows La K-edge XANES spectra of 0.1 and 3.4 mmol La/Al_2O_3. In an ex-situ condition, 0.1 mmol La/Al_2O_3 gave a XANES spectrum identical to that of $La(OH)_3$ or $La_2(CO_3)_3{\cdot}8H_2O$. Spectra of both La/Al_2O_3 catalysts calcined at 873 K were similar to those of II-$La_2O_2CO_3$ and La_2O_3, but quite different from those of lanthanum−aluminum binary oxides ($LaAlO_3$ and $LaAl_{11}O_{18}$). The drastic change upon calcination at 1273 K should be noted. The XANES spectrum of 0.1 mmol La/Al_2O_3 was little changed by thermal treatment,

(61) Malet, P.; Benitez, J. J.; Capitan, M. J.; Centeno, M. A.; Carrizosa, I.; Odriozola, J. A. *Catal. Lett.* **1993**, *18*, 81−97.

(62) Shinn, D. B.; Eick, H. A. *Inorg. Chem.* **1968**, *7*, 1340−1345.

(63) Krause, M. O.; Oliver, J. H. *J. Phys. Chem. Ref. Data* **1979**, *8*, 329−338.

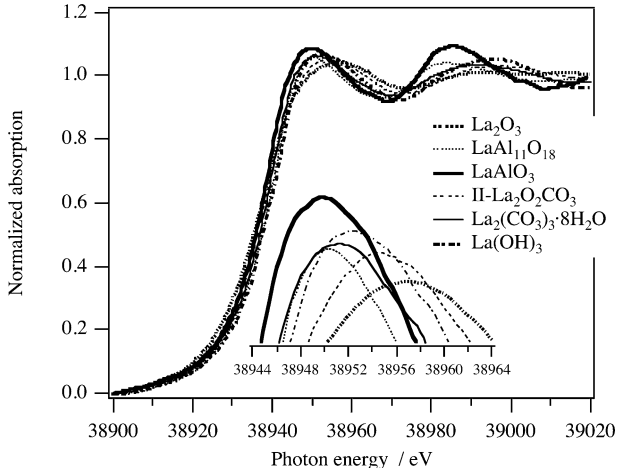

Figure 10. La K-edge XANES spectra of reference compounds.

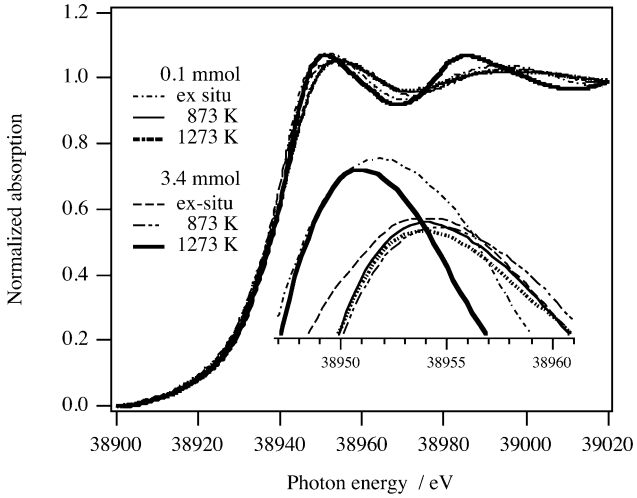

Figure 11. La K-edge XANES spectra of 0.1 and 3.4 mmol La/Al_2O_3 with different calcination temperatures.

whereas 3.4 mmol La/Al_2O_3 exhibited spectra identical to that of $LaAlO_3$. The local structure and symmetry around La species on 0.1 mmol La/Al_2O_3 were little changed by thermal treatment, i.e., $LaAlO_3$ crystallites never form on La/Al_2O_3 at a low loading amount of 0.1 mmol $g(Al_2O_3)^{-1}$ (1.6 wt % as La_2O_3).

Figure 12 shows XANES spectra of La/Al_2O_3 calcined at 1273 K. In the case of other calcined samples with different loadings, the spectral feature of XANES spectra gradually changed by thermal treatment at 1273 K with loading amount. Here, we propose that only aggregated La species on Al_2O_3 transformed to the $LaAlO_3$ binary oxide phase by thermal treatment below 1273 K, and isolated ones retained the original oxide-like structure after thermal treatment, as well as the case of Cu/Al_2O_3 system.[64] Then, we carried out convolution analysis of XANES spectra with two standard spectra.[65−67] The one is that of $LaAlO_3$, the another is

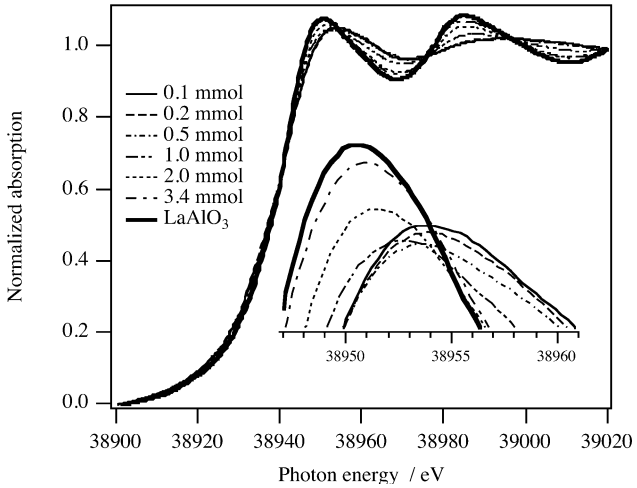

Figure 12. La K-edge XANES spectra of La/Al_2O_3 calcined at 1273 K.

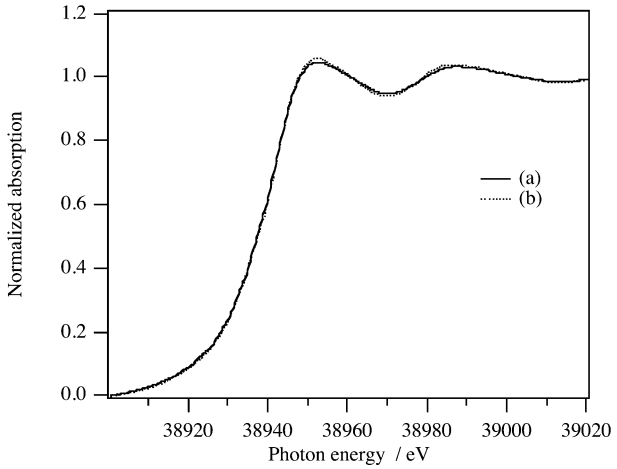

Figure 13. La K-edge XANES spectrum of 1.0 mmol La/Al_2O_3 calcined at 1273 K (a); and convoluted spectrum (b) (= 0.60*A* + 0.40*B*; where *A* = 0.1 mmol La/Al_2O_3 calcined at 873 K and B = $LaAlO_3$.

that of isolated one. As for a standard spectrum for isolated La species, we adopted that of 0.1 mmol La/Al_2O_3 treated at 873 K. As expected, all XANES spectra of La/Al_2O_3 treated at 1273 K could be reproduced with the isolate-standard spectrum and that of $LaAlO_3$. As example, Figure 13 shows results of convolution analysis for 1.0 mmol La/Al_2O_3. Fractions of $LaAlO_3$ phase were estimated to be 85, 65, 40, and 12% for 3.4, 2.0, 1.0, and 0.5 mmol La/Al_2O_3 treated at 1273 K, respectively. These values directly indicate the fraction of aggregates to all La species on Al_2O_3. A fraction of aggregated La species increased with loadings, and a threshold for the aggregation was 0.5 mmol La $g(Al_2O_3)^{-1}$ (7.5 wt % as La_2O_3). On the other hand, XANES spectra of 0.2 and 0.1 mmol La/Al_2O_3 treated at 1273 K were almost identical to that of the isolated standard spectrum. This effectively demonstrates that the isolated La species does not transform to $LaAlO_3$ perovskite phase at 1273 K.

Structures of La Species on Al_2O_3. As shown in Table 1, estimated averages of La concentrations for 0.1 and 3.4 mmol La/Al_2O_3 are 0.36 and 28 La atom nm^{-2}, respectively. Using ionic radii of La^{3+} and O^{2-}, we estimate the occupied area for one LaO_x to be 0.20 nm^2. This shows that 5 La atoms nm^{-2} corresponds to

(64) Yamamoto, T.; Tanaka, T.; Suzuki, S.; Kuma, R.; Teramura, K.; Kou, Y.; Funabiki, T.; Yoshida, S. *Top. Catal.* **2002**, *18*, 113−118.
(65) Tanaka, T.; Yamamoto, T.; Kohno, Y.; Yoshida, T.; Yoshida, S. *Jpn. J. Appl. Phys. Part 1* **1999**, *38*, 30−35.
(66) Yoshida, S.; Tanaka, T.; Hanada, T.; Hiraiwa, T.; Kanai, H.; Funabiki, T. *Catal. Lett.* **1992**, *12*, 277−286.
(67) Yoshida, S.; Tanaka, T. In *X-ray Absorption Fine Structure for Catalysts and Surfaces*; Iwasawa, Y., Ed.; World Scientific: Singapore, 1996; pp 304−325.

formation of a LaO_x monolayer on a catalyst surface, if it forms. Then, we conclude that La species in 0.1 mmol La/Al_2O_3 were supported on Al_2O_3 in a highly dispersed form, and those in 3.4 mmol La/Al_2O_3 formed an aggregated one.

In an ex situ condition, 0.1 mmol La/Al_2O_3 gave a XANES spectrum identical to that of $La(OH)_3$ or $La_2(CO_3)_3 \cdot 8H_2O$. The EXAFS parameters are similar to those of both of $La(OH)_3$ and $La_2(CO_3)_3 \cdot 8H_2O$. However, amplitude of the EXAFS spectrum of $La(OH)_3$ and the first peak in the RSF are stronger than those for $La_2(CO_3)_3 \cdot 8H_2O$. IR characterization demonstrates the existence of carbonate species. Therefore, we conclude that La species on Al_2O_3 are present as carbonate hydrates under exposure to the air.

As discussed above, the present estimated coordination numbers for La−O pair in La/Al_2O_3 (ca. 4) do not always mean that the supported La species exists as a LaO_4 tetrahedron. As shown in Figures 8 and 9, EXAFS spectra of low-loading samples give a beat-node (k_{node}) around 8.5 $Å^{-1}$. Since the beat results from the simple sum of plural sine waves at different frequencies, the beat in the oscillation indicates the existence of at least two kinds of La−O bonds. Assuming that two La−O bonds are present, the difference of the bond distance, Δr, can be estimated to be 0.18 Å using the following equation: $k_{node}\,\Delta r = \pi/2$.[68] If it can be applied to this system, it is possible that the other La−O bonding with long bond length, ca. 2.70 Å, exists. In fact, La L_{III} edge EXAFS analysis for 10 wt % La/Al_2O_3 suggests the existence of two kinds of La−O bonds (2.50 and 2.71 Å).[60,61] However, multielectron excitation strongly affects the La L_{III} edge-EXAFS spectrum, especially in the present La/Al_2O_3 system.[33,61] Because of a narrow EXAFS range due to the limit by L_{II} edge and strong multielectron excitation, reliability of curve-fitting analysis for La L_{III} edge EXAFS against amorphous system is not so high. Therefore, we are not sure whether long La−O bonds (ca. 2.70 Å) accompany short La−O bonds (ca. 2.50 Å). The point of the present curve-fitting analysis is that lanthanum hydroxide or carbonate-like species decompose (or change the local structure) by calcination at 873 K, and form shorter La−O bonding.

It should be noted that 0.1 and 0.2 mmol La/Al_2O_3 calcined at 1273 K gave EXAFS parameters similat to those calcined at 873 K, although the Debye−Waller factors became somewhat large. This shows that the coordination environment of La species on low-loading La/Al_2O_3 did not change by thermal treatment below 1273 K, in contrast to the higher loading sample above 0.5 mmol $g(Al_2O_3)^{-1}$. After calcination, the carbonate-like species decomposed to form oxide-like species. IR characterization of adsorbed pyridine demonstrates that addition of La to γ-Al_2O_3 titrates the original strong Lewis acid site and forms weaker Lewis acid sites. The coordinatively unsaturated Al atoms in γ-Al_2O_3 act as a Lewis acid site. We propose that the La atom is located on the unsaturated Al atom via an oxygen atom, as shown in Figure 14. At higher concentration above 0.5 mmol La/Al_2O_3, some La species form aggregates which easily transform to $LaAlO_3$.

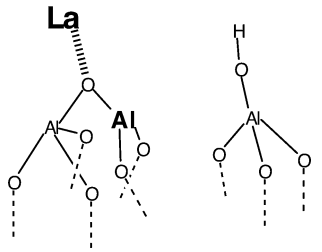

Figure 14. Proposed structure of La species on acid site of γ-Al_2O_3.

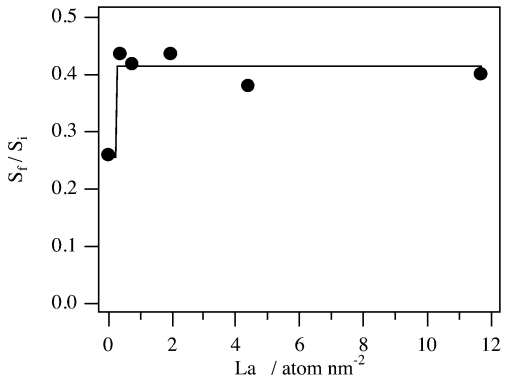

Figure 15. Relative surface area loss of La/Al_2O_3. S_i: BET specific surface area of La/Al_2O_3 calcined at 873 K. S_f: BET specific surface area of La/Al_2O_3 calcined at 1273 K.

(3) Effect of La Addition to Alumina Against Sintering. Figure 15 shows relative surface area loss of La/Al_2O_3 by calcination at 1423 K (sintered sample). Without addition of La, the surface area of the sintered sample was 26% of the original. On the other hand, surface areas of La-promoted samples retained about 40% of their original size. It should be noted that the promotion effect was independent of the loaded amount, and saturated even at a low density of 0.36 La atom nm^{-2}. XRD characterization revealed that the Al_2O_3 phase of sintered sample without La was α-phase, but those with La were δ-phase. At higher concentration, above 1.97 La atom nm^{-2} (0.5 mmol La $g(Al_2O_3)^{-1}$), $LaAlO_3$ crystallite formed on sintered samples, showing that addition of La suppresses the phase transformation of alumina not from γ- to δ-phase, but from δ- to α-phase. These phenomena are consistent with previous reports.[7,9,14,16] XRD and XAFS characterization revealed that no $LaAlO_3$ perovskite formed in the case of the low concentration. We conclude that formation of $LaAlO_3$ perovskite on Al_2O_3 surface is not a key point to enhance thermal stability of alumina-based catalyst.

As for enhancement of thermal stability of Al_2O_3, we assume that the key point is to poison the strong Lewis acid site of γ-Al_2O_3. It is well-known that the existence of H_2O enhances progressing of sintering.[1] Here, we propose a sintering mechanism of γ-Al_2O_3 as shown in Scheme 1. First, coordinatively unsaturated Al (I) reacts with H_2O, and the Al−O−Al bond is hydrolyzed to form surface hydroxyl groups (II). Second, surface hydroxyl groups are removed by dehydration to form Al−O−Al linkage (I or III). If the dehydration procedure goes along the orientation toward III, this means that the coordinatively unsaturated Al−O linkage moves to another place. At high temperature with H_2O vapor, these two steps occur repeatedly and rapidly, bringing about that the surface area would be drastically re-

(68) Martens, G.; Rabe, P.; Schwentner, N.; Werner, A. *Phys. Rev. Lett.* **1977**, *39*, 1411.

Scheme 1 Proposed Sintering Mechanism of γ-Al_2O_3

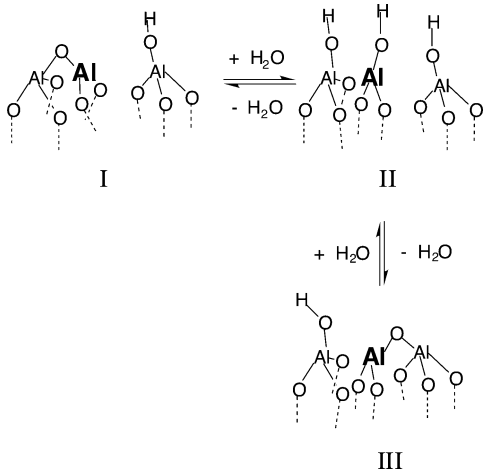

duced, and finally the phase transforms to α-Al_2O_3. It has been reported that phase transformation of Al_2O_3 to α-phase is accompanied with dehydroxylation process.[1,2,4] However, no one has considered the effects of acid−base properties of catalyst surfaces on a mechanism for sintering. In a case for La/Al_2O_3, strong Lewis acid sites of γ-Al_2O_3 were titrated by La atoms, and such a hydrolysis−dehydration cycle would be greatly suppressed. Consequently, La/Al_2O_3 exhibits higher thermal stability than Al_2O_3 itself. This sintering mechanism is supported by the result that extent of surface area reduction of γ-Al_2O_3 is quite different between the conditions under the presence and the absence of H_2O. Figure 16 shows the result. Under 2.67 kPa of H_2O, γ-Al_2O_3 was losing surface area even at 1073 K. On the other hand, sintering was drastically suppressed in the absence of H_2O.

Conclusions

The La addition to Al_2O_3 suppresses sintering even at a low concentration of 0.1 mmol La g$(Al_2O_3)^{-1}$ (1.6 wt % as La_2O_3, 0.36 La atom nm^{-2}). The Al−O−Al linkage of strong Lewis acid site (coordinately unsaturated Al sites) is hydrolyzed at high temperature in the presence of H_2O, and dehydrated to form another Al−O−Al linkage. Sintering of γ-Al_2O_3 proceeded via transportation of the coordinatively unsaturated Al sites. The addition of La to γ-Al_2O_3 poisons the original strong acid sites and generates other weaker Lewis acid sites. Titration of strong Lewis acid sites on Al_2O_3 suppresses the hydrolysis−dehydration scheme, resulting in retarding the phase transformation from δ- to α-phase. The formation of $LaAlO_3$ perovskite phase on the surface of Al_2O_3 is not related with the enhancement of the thermal stability.

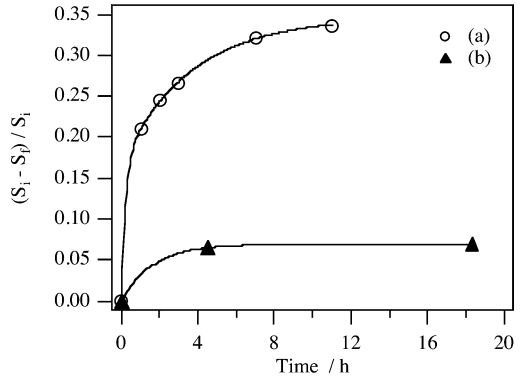

Figure 16. Surface area reduction of γ-Al_2O_3 after calcination at 1073 K under 2.7 kPa of H_2O (a) and dry He (b).

Supported La species on Al_2O_3 exist as carbonate hydrate under exposure to the air, but decompose after calcination at 873 K. Isolated La species on Al_2O_3 do not change their local structure after calcination at 1273 K, but aggregated species easily form $LaAlO_3$ even at 1073 K. Fractions of aggregated species to isolated species could be quantified by convolution analysis of XANES spectra calcined at 1273 K.

Acknowledgment. We thank Drs. H. Tanida and T. Uruga (Japan Synchrotron Radiation Research Institute, SPring-8) for carrying out the X-ray absorption experiments. The X-ray absorption experiments have been performed under the approval of the JASRI (Proposal 2000A0059). Japan Reference Catalysts (JRC) were supplied by the Committee on Reference Catalyst, Catalysis Society of Japan. This work was partially supported by a grant-in-aid from the Japan Ministry of Education, Science, Sports, and Culture. T.Y. acknowledges support by JSPS Research Fellowships for Young Scientists.

CM034732C